

Molecular Crystals and Liquid Crystals Science and Technology. Section A. Molecular Crystals and Liquid Crystals

Publication details, including instructions for authors and
subscription information:

<http://www.tandfonline.com/loi/gmcl19>

ENDOR and EPR of a Nitroxyl Radical Formed from N,2,4,6-Tetranitro-N- Methylaniline

M. D. Pace^a & R. Weber^b

^a Code 6122, Naval Research Laboratory, Washington, D.C.,
20375-5000

^b Bruker Instruments, Inc., Manning Park, Billerica, Mass, 01821
Version of record first published: 24 Sep 2006.

To cite this article: M. D. Pace & R. Weber (1992): ENDOR and EPR of a Nitroxyl Radical Formed from N,2,4,6-Tetranitro-N-Methylaniline, Molecular Crystals and Liquid Crystals Science and Technology. Section A. Molecular Crystals and Liquid Crystals, 214:1, 189-202

To link to this article: <http://dx.doi.org/10.1080/10587259208037293>

PLEASE SCROLL DOWN FOR ARTICLE

Full terms and conditions of use: <http://www.tandfonline.com/page/terms-and-conditions>

This article may be used for research, teaching, and private study purposes. Any substantial or systematic reproduction, redistribution, reselling, loan, sub-licensing, systematic supply, or distribution in any form to anyone is expressly forbidden.

The publisher does not give any warranty express or implied or make any representation that the contents will be complete or accurate or up to date. The accuracy of any instructions, formulae, and drug doses should be independently verified with primary sources. The publisher shall not be liable for any loss, actions, claims, proceedings, demand, or costs or damages whatsoever or howsoever caused arising directly or indirectly in connection with or arising out of the use of this material.

ENDOR and EPR of a Nitroxyl Radical Formed from N,2,4,6-Tetranitro-N-Methylaniline

M. D. PACE

Code 6122, Naval Research Laboratory, Washington, D. C. 20375-5000

and

R. WEBER

Bruker Instruments, Inc., Manning Park, Billerica, Mass. 01821

(Received August 31, 1991; in final form November 26, 1991)

ENDOR (electron-nuclear double resonance) spectra of 2,4,6-tetranitrophenyl-N-methylnitroxyl radical (I) in N,2,4,6-tetranitrophenyl-N-methylaniline (tetryl; $C_7N_5H_5O_8$) are recorded at 120 K and 4 K. At 120 K, an ENDOR signal at 28.3 MHz is observed and assigned to the β -proton couplings of the $-\text{CH}_3$ group. At 4 K, matrix ENDOR signals are detected at 14.5 MHz due to an unknown trapped species (possibly $\cdot\text{CH}_3$ or $\cdot\text{NO}$). Also at 4 K, signals are assigned to the ^1H atoms of the nitroaromatic ring. A computer model based on the crystal structure coordinates reveals that (I) retains the parent molecule configuration of tetryl. The principal g-values of (I) determined by a single crystal EPR (electron paramagnetic resonance) study at 298 K are: $g_x = 2.0088$, $g_y = 2.0060$, $g_z = 2.0020$. The principal ^{14}N hyperfine couplings (hfc) are: $A_x = 0.125$ mT, $A_y = 0.425$ mT, $A_z = 2.78$ mT. The principal ^1H hfc are nearly isotropic due to rotation of the $-\text{CH}_3$ group with values: $A_x = 1.2$ mT, $A_y = 1.0$ mT, $A_z = 1.0$ mT. The highly stable nature of (I) in tetryl and the insensitivity of tetryl suggests that *stable* nitroxyl radicals in energetic materials may be *indicators* of mechanical and thermal sensitivity.

I. INTRODUCTION

N,2,4,6-tetranitro-N-methylaniline (tetryl; $C_7N_5H_5O_8$), prepared by the nitration of dimethylaniline, is an energetic material which has been used since 1906.¹ Tetryl converts to a room temperature stable nitroxyl radical, 2,4,6-trinitrophenyl-N-methylnitroxyl (I) upon exposure to 250–360 nm light in either the solution phase or the solid phase. Free radical (I) was first studied by Owens.² The EPR (electron paramagnetic resonance) spectrum of (I) dissolved in benzene at 298 K is assigned to two hyperfine couplings: an isotropic ^{14}N coupling and a $-\text{CH}_3$ group isotropic proton coupling, both equal to 1.0 mT (Figure 1a). In solution, (I) gradually decays, but when formed in a single crystal, radical (I) is highly stable with no evidence of decay even after several months at ambient temperature and pressure.

We have noticed that low concentrations of (I) exist in some tetryl samples even

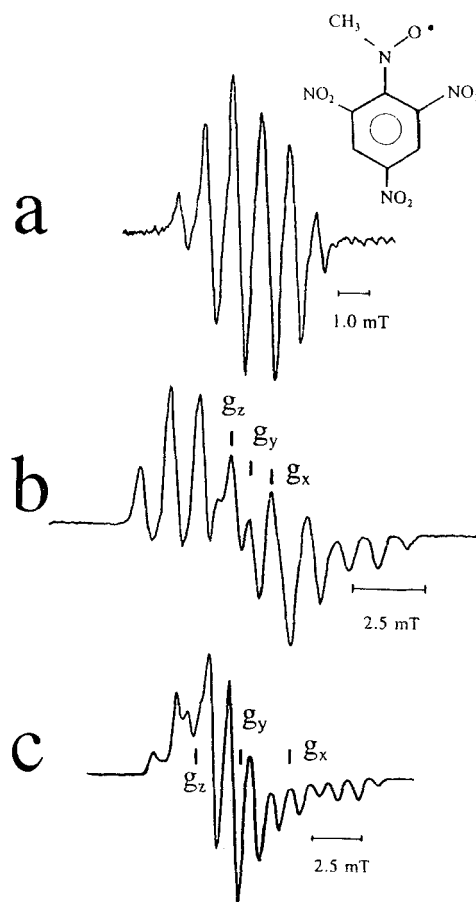


FIGURE 1 (a) The X-band spectrum of radical (I) (structure shown) in toluene at room temperature. The pattern is assigned to an ^{14}N hyperfine coupling and three equivalent ^1H couplings, equal to 1.0 mT for each type of coupling. The parent tetryl molecule differs from the radical by replacement of NO_2 for O in the $-\text{N}-\text{O}\cdot$ functional group. (b) The X-band (9.5 GHz) polycrystalline EPR spectrum of (I). g_x , g_y , g_z are indicated. (c) The calculated Q-band (35 GHz) polycrystalline EPR spectrum of (I). g_x , g_y , g_z are shifted relative to the X-band spectrum (b), but not completely resolved.

without exposure to ultraviolet (uv) light. For example, Figure 1b shows the EPR spectrum of powdered tetryl without prior uv-irradiation. The estimated free radical concentration of this signal is 150 ppm based on sample weight. Past studies have established that there is a relationship between molecular structure and sensitivity of certain energetic materials.^{3,4} (Here, sensitivity refers to shock-impact measurements of high-energy materials partially governed by thermal decomposition reactions generated by an impacting weight. The height which gives 50% probability of detonation is the measure of sensitivity.) The relationship between impurities, particularly free radical impurities, and inherent sensitivities of energetic materials has not been studied in detail. The detection and characterization of free radicals such as (I) is part of an effort to understand whether or not free radicals can influence sensitivity. The purpose of this EPR/ENDOR experiment is to study the

electronic structure of (I) in the solid-state in order to understand what factors contribute to stability. First, a single crystal EPR experiment at X-band is reported, with supporting Q-band EPR measurements. A complete single crystal analysis has not been previously attempted because the EPR spectra of (I) in single crystals of tetryl are unusually complicated due to site splitting. Second, X-band ENDOR analysis of single crystal and polycrystalline tetryl samples at temperatures of 4 K, 120 K, and room temperature show hyperfine couplings and motional properties of (I) not accessible by EPR. The EPR/ENDOR results of this radical system demonstrate: (i) the first ENDOR spectra of an energetic material, (ii) methyl group rotation in the solid-state, and (iii) β -proton hyperfine coupling (hfc) interactions with a nitroxyl group.

II. EXPERIMENTAL

Tetryl was supplied by Sharma of the Naval Surface Warfare Center, White Oak, MD. The sample was studied as received, yielding EPR signals of (I) as impurities, and also was recrystallized from toluene to form single crystals. Recrystallization from toluene did not remove the radical impurities. This was not surprising since previous solution phase EPR studies of (I) in benzene detected stable radicals at room temperature. The crystal structure of tetryl has been reported by Cady.⁵ For most studies, no ultraviolet light (uv) was needed to form (I); however, to increase the concentration of (I), giving better spectral signal-to-noise (S/N) ratio, a 1000 watt Hg-Xe Hanovia (Electro Powerpacs Inc., Cambridge, MA) high pressure arc lamp was used. Broad-band uv irradiation of the sample for 30 minutes at room temperature typically improved the S/N ratio by an order of magnitude. No attempt was made to quantify the quantum yields in this experiment since the purpose of the study was to characterize the radical stability.

The ENDOR and EPR spectra were first recorded at Bruker Instruments, Inc., Billerica, MA, using an ESP 300 spectrometer and ENDOR accessory and an Oxford ESR 900 cryostat for helium temperature measurements.* Subsequently, the ENDOR results were reproduced at the Naval Research Laboratory (NRL), Washington, D. C., using a Bruker ER 200 with ENDOR accessory. ENDOR spectra of polycrystalline tetryl samples were also recorded at the University of Alabama, Tuscaloosa, AL, Chemistry facility. A Q-band spectrum was recorded using a Varian E-Series spectrometer at NRL. Simulated spectra were produced using the Chemistry VAX-11 computer at NRL. The software was adapted from an EPR program written at NRL for studying organometallic thin films.⁶

III. SINGLE CRYSTAL EPR AND SPECTRAL SIMULATION

Tetryl has a monoclinic unit cell with space group $P2_1/c$ and four molecular sites per unit cell ($a = 1.412$ nm, $b = 0.7374$ nm, $c = 1.0614$ nm, $\beta = 95.07^\circ$).⁵ The

*Commercial references for identification purposes only.

four sites are related by the coordinate transformations (x,y,z) , $(-x,-y,-z)$, $(x,0.5 + y,0.5 - z)$, and $(-x,0.5 - y,0.5 + z)$. Because the sites are related pairwise by inversion symmetry, there are two congruent but magnetically distinguishable sites in the solid-state EPR spectra. This site multiplicity causes a severely congested EPR spectrum if a symmetry axis is not parallel to \mathbf{B}_0 (the applied magnetic field) because each radical site can have 12 EPR lines (assuming equivalence of the methyl protons). These overlapping transitions make spectral interpretations very difficult, even when the rotational anisotropy of each transition is carefully mapped. This difficulty was overcome by using a computer model to simulate the EPR spectra.

The modeling protocol was to first construct the geometry of (I) using the crystal structure coordinates of tetryl, then to assign approximations of the g -values and ^1H and ^{14}N hyperfine couplings based on the experimental solution-phase and polycrystalline phase EPR spectra. A "single crystal" EPR spectrum was then simulated by calculating and summing spectra of all symmetry related sites of (I) in the unit cell. This procedure was repeated for variations of \mathbf{B}_0 to build a set of simulated single crystal spectra.

First-approximations of the principal g -values and the hyperfine couplings of (I) were measured from the solution spectrum and the X-band and Q-band polycrystalline spectra (Figure 1). Table I gives the final g and hfc assignments of these spectra. Our maximum ^{14}N hfc and g -values agree with those measured by Owens. The smaller numbers in Table I, corresponding to $^N A_x$, $^N A_y$, g_y , and g_z , are difficult to measure directly from the spectra, even at Q-band frequency. For this reason, careful comparison of simulated and experimental EPR spectra, while varying g_y , g_z , $^N A_x$, and $^N A_y$, was necessary in order to achieve a high level-of-confidence of these assignments. The ^1H hfc values are found to be nearly isotropic due to methyl group rotation. This is discussed in section IV. The next paragraph gives a detailed description of the computer model.

The molecular structure of radical (I) is derived from the parent tetryl molecule by substituting oxygen in place of NO_2 in the nitramine functional group. Experimentally this substitution has been observed in thermal and photolytic reactions of other high-energy nitro-compounds.⁷ The unit cell coordinates of the tetryl crystal structure are transformed from the monoclinic system into an orthogonal abc^*

TABLE I
 ^{14}N , ^1H Hyperfine couplings and g -values of (I)

<u>This study:</u>			
	$g_x = 2.0088$	$g_y = 2.0060$	$g_z = 2.0020$
^{14}N	$A_x = 0.125 \text{ mT}$	$A_y = 0.425 \text{ mT}$	$A_z = 2.78 \text{ mT}$
^1H	$A_x = 1.2 \text{ mT}$	$A_y = 1.0 \text{ mT}$	$A_z = 1.0 \text{ mT}$
<u>Reference 2:</u>			
	$g_x = 2.0071$	$g_y = g_z = 2.0039$	
^{14}N	$A_x = A_y = 0.4 \text{ mT}$	$A_z = 2.75 \text{ mT}$	
^1H	$A_x = 1.0 \text{ mT}$	$A_y = 1.0 \text{ mT}$	$A_z = 1.0 \text{ mT}$

molecular system where a and b coincide with the unit cell axes and c^* is orthogonal to the ab plane.⁸ A molecular reference frame is assigned to the resulting nitroxyl group as follows (Figure 2): the X -axis direction is along the nitrogen-oxygen bond, the Y direction is perpendicular to the plane formed by X and Z , the Z direction is perpendicular to the XY plane defined by the methyl carbon, nitroxyl nitrogen, and ring carbon of $\text{H}_3\text{C}-(\text{NO}\bullet)-\text{C}_6\text{H}_2(\text{NO}_2)_3$. The direction cosines of X , Y , and Z are calculated from the abc^* coordinates (Table II). These direction cosines are used in the computer simulation to specify the directions of the principal g -values and hyperfine couplings. From many previous studies we know that nitroxyl radicals have typical values of $g_x = 2.009$, $g_y = 2.006$, and $g_z = 2.002$ and $^N A_x = 0.6$ mT, $^N A_y = 0.6$ mT, and $^N A_z = 3.2$ mT.⁹ Based on this first-order data, approximate values were assigned to the directions in Table II. This formed the basis for calculation of the EPR spectra and refinement of the g -values and hyperfine couplings.

The interpretation of single crystal EPR spectra depends on the correlation

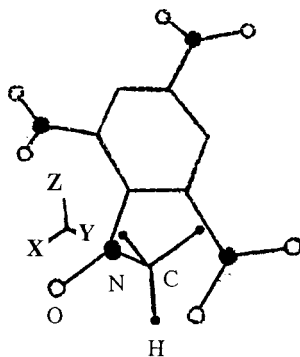


FIGURE 2 This figure shows a ball-and-stick model of the molecular structure of (I) based on the crystal structure coordinates. The XYZ molecular reference frame is indicated with: X along the $\text{N}-\text{O}$ bond; Y orthogonal to X and Z ; and the Z axis perpendicular to the plane defined by three atoms: the carbon of the CH_3 , the nitrogen of the nitroxyl group, and the ring carbon to which the methyl-nitroxyl group is attached. The nitrogen atoms are indicated by large darkened circles, the oxygens by open circles, and the CH_3 hydrogens by small darkened circles. This reference system was used for the spectral simulations.

TABLE II

Direction cosines of the XYZ molecular reference frame
calculated from the crystal structure

Axis	Direction Cosines ^a		
X	(0.360	0.278	-0.891)
Y	(0.918	-0.274	0.286)
Z	(0.164	0.921	0.354)

^aDirection cosines for site XYZ only; XYZ defined in Figure 2.

between the crystal axes and the laboratory reference frame; which in this case is the abc^* frame. Fortunately, our first-order values are very close to the final refined values. The large ^{14}N $h\nu$ anisotropy causes distinct differences in the spectral patterns for \mathbf{B}_0 along a , b , or c^* , making match with experimental spectra unambiguous. Also for \mathbf{B}_0 along the a, b, c^* axes the EPR spectra are not complicated by site splitting. The calculated and experimental spectra along these axes are in excellent agreement (see spectra, Figure 3), supporting the following conclusions: (i) The formation of (I) in the solid occurs with no reorientation of the parent molecule, and (ii) the axes a and b are correctly assigned to the tetryl crystal (otherwise, the experimental and calculated spectra would not coincide). Final confirmation of axes requires correlation with X-ray diffraction data; therefore, these assignments are considered 'pseudo' axes.

IV. METHYL GROUP ROTATION

At this point it is important to note that at temperatures above 4 K the $-\text{CH}_3$ group of (I) is freely rotating in the tetryl crystalline solid on the EPR timescale.

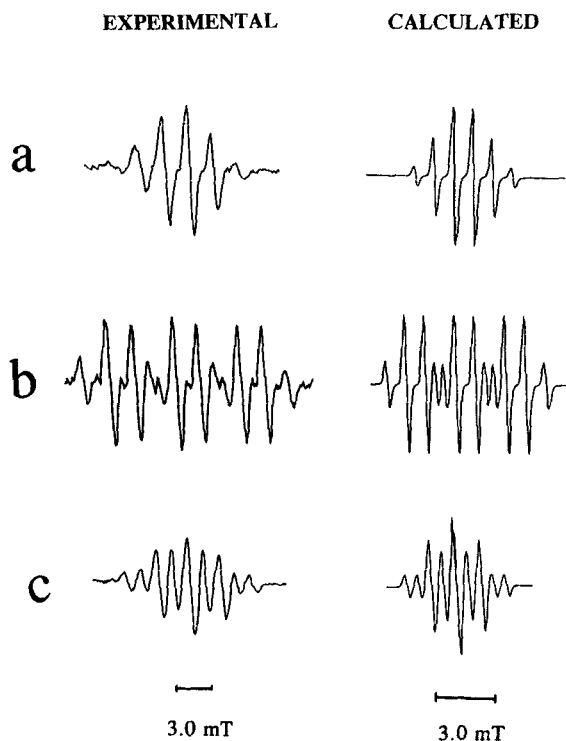


FIGURE 3 The experimental and simulated single crystal EPR spectra of (I) in the abc^* lab reference frame (based on the molecular XYZ assignments in Figure 2) for: (a) \mathbf{B}_0 along the c^* axis, (b) \mathbf{B}_0 along the b axis, (c) \mathbf{B}_0 along the a axis. The values in Table I and the direction cosines in Table II were used in the simulations.

How do we know this? The first evidence is the crystal structure. X-ray diffraction studies indicate a large spread in the dihedral angles of the CH_3 group protons. This means a high degree of disorder, suggesting motion. The second evidence is the β -hyperfine couplings and intensity ratios measured from the EPR spectra. For example, for \mathbf{B}_0 along the b axis (Figures 3b and 3e) the EPR spectrum is a triplet of quartets. Each quartet has an intensity ratio of 1:3:3:1 as expected for motionally averaged $-\text{CH}_3$ group proton hyperfine couplings. The β -proton hfc of the quartet is ≈ 1.0 mT in all single crystal EPR spectra at 77 K. This is the isotropic value observed for (I) in benzene solution at room temperature, consistent with findings by Owens.² The β -proton hyperfine couplings are given by:

$$a^H = B_0 + B_1 \langle \cos \theta \rangle + B_2 \langle \cos^2 \theta \rangle \quad (1)$$

Here, θ is the dihedral angle between the $-\text{N}-\text{C}-\text{H}_i$ plane and the p -orbital of the $-\text{NO}\cdot$ functional group (the Z axis in Figure 2) and the time-averaged expectation values are determined by $\langle \cos \theta \rangle$, which for rotation of 2π approaches zero, and $\langle \cos^2 \theta \rangle$. The values of a^H (a indicates isotropic hfc) have been measured by Maender and Janzen for a series of trityl alkyl nitroxides with β -methylene couplings: $(\text{C}_6\text{H}_5)_3\text{C}-(\text{NO}\cdot)-X$, where $X = -\text{CH}_3$, $-\text{CH}_2R$, with $R =$ various alkyl groups.¹⁰ From their solution phase studies with $X = \text{CH}_3$, $a_\beta^H = 0.996$ mT, identical within experimental error to the solution phase value measured for (I). Several other studies of hindered motion of substituted methyl groups of alkyl radicals have attempted to determine values of B_0 and B_2 .¹¹ For alkyl radicals B_2 values range from 4.0–5.0 mT. A very simple estimate of B_2 can be made for (I) according to equation (1), i.e., $B_2 = 1.0 \text{ mT} / \langle \cos^2 \theta \rangle$, assuming $B_0 \approx 0$ since $B_0 \ll B_2$. For a freely rotating methyl group $\langle \cos^2 \theta \rangle = 0.5$, yielding $B_2 = 2$ mT. This value is half the minimum value of B_2 measured for alkyl radicals. The shared spin density distribution of the nitroxyl group between nitrogen and oxygen may account for this. For this study we assume the partitioning of spin density of the nitroxyl group is $0.5 \rho_T$ on nitrogen and $0.5 \rho_T$ on oxygen where $\rho_T =$ the total unpaired electron spin density.¹² This means that the magnitude of the rotationally averaged interactions between the β protons and the spin density in the p -orbital of the nitrogen is approximately half that of alkyl radicals. This would equal the observed value of 1.0 mT for $B_2 = 2$ mT and $B_0 = 0$. Careful temperature dependent measurements are required to arrive at precise values of B_2 and this is reserved for future study. For this study, the critical point has been discussed; namely, that the $-\text{CH}_3$ group freely rotates in the solid-state except at very low temperatures.

V. ENDOR MEASUREMENTS

Now that the EPR spectra have been described, the ENDOR spectra are easier to understand. A single crystal of tetryl was aligned with \mathbf{B}_0 near the b axis. This spectrum is shown in Figure 4a. The intensities of the low field and center field transitions of the EPR signal, corresponding to ^{14}N , $m_I = -1$ and $m_I = 0$ spin

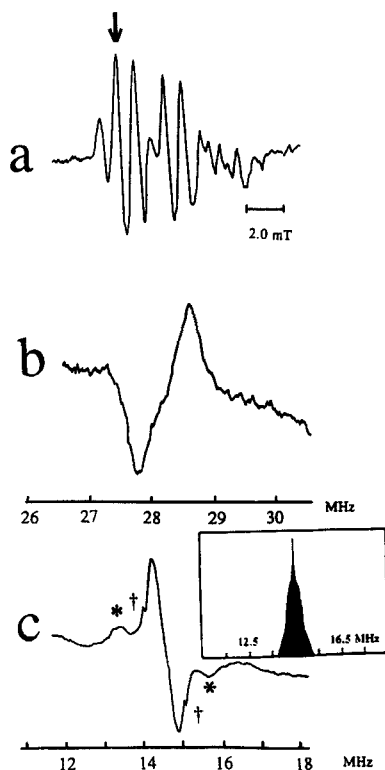


FIGURE 4 (a) X-band EPR of \mathbf{B}_0 near the (0,1,0) tetryl crystal axis. This spectrum was recorded at 120 K. The \mathbf{B}_0 magnetic field was locked at the transition indicated by the arrow for ENDOR measurements. (b) This ENDOR spectrum was recorded at 120 K for the crystal orientation in Figure 4(a) using the following settings: rf modulation, 500 kHz. The microwave power was 10 milliwatts. (c) This ENDOR spectrum of the crystal orientation in 4(a) was recorded at 4 K using settings as indicated in (b). The peaks labeled * are assigned to small aromatic ring proton couplings. The peaks labeled † and the center peak are assigned to matrix ENDOR signals. The inset shows a calculated *absorption* lineshape predicted by equation 4 for a dipolar interaction of 50 kHz and a linewidth of 10 kHz. The calculation was for r_i from 1 nm to 100 nm from the paramagnetic center. Although the fit is not exact, the calculation shows that flanking peaks as indicated by the † are predicted.

manifolds are maximized. Since for the spectrum in Figure 4a the crystal was not perfectly aligned along the b axis, the $m_I = +1$ ^{14}N transitions in Figure 4a are weaker than the $m_I = -1$ or $m_I = 0$ transitions. For the ENDOR experiments, one of the $m_I = -1$ transitions indicated by the arrow (Figure 4a) was saturated by microwave power. ENDOR is particularly sensitive to the electron spin relaxation properties of the sample and at room temperature where T_{1e} (the electron spin-lattice relaxation time) is fast, no signals were detected.

An ENDOR signal was detected at 120 K, centered at 28.3 MHz (Figure 4b). No other signals were detected within the range of 10–30 MHz or below 10 MHz at 120 K. The signal at 28.3 MHz is symmetrical and has a peak-to-peak width of approximately 0.8 MHz. There are two nuclei, ^1H and ^{14}N , which might account for this ENDOR signal. At the magnetic field setting of 340 mT the nuclear fre-

quency for ^1H nuclei is $\nu_n = 14.5$ MHz and for ^{14}N nuclei, $\nu_n = 1.05$ MHz. To understand which of these nuclei account for this spectrum, we examine the three general cases for ENDOR¹³: (i) For the nuclear frequency greater than half the hyperfine coupling ($\nu_n > |A|/2$) two ENDOR signals centered at ν_n are predicted with frequencies given by $\nu_n \pm |A|/2$; (ii) for $\nu_n < |A|/2$ the ENDOR transitions are given by $|A|/2 \pm \nu_n$ and centered at $|A|/2$ and (iii) for $\nu_n = |A|/2$ only one ENDOR line is observed at $\nu_n + |A|/2$.

If this signal is attributed to ^{14}N , then case (ii) obtains and the observed signal would be centered at half the ^{14}N hyperfine coupling, since $|A|/2 > \nu_n$. Therefore, the ^{14}N hyperfine coupling would have to equal 2×28.3 MHz or 2.02 mT (56.6 MHz). From the EPR spectrum it is possible to measure the ^{14}N hyperfine coupling between the low field and center field lines at this orientation. The ^{14}N hyperfine coupling measured from the EPR spectrum is 2.65 mT (74 MHz) which does not match the value needed for an ^{14}N assignment. Furthermore, there should be a large dependence of the ^{14}N coupling on the orientation of the crystal. To check this, the crystal was reoriented with \mathbf{B}_0 along the c^* axis where $A(^{14}\text{N}) = 0.64$ mT (18 MHz). An ENDOR spectrum recorded at this orientation gave a signal at 28.3 MHz.

The ENDOR spectrum of tetryl powder was also recorded at 120 K. This spectrum is not shown but, as in the single crystal study, a transition is observed at 28.3 MHz. The 28.3 MHz signal is observed consistently at 120 K in both powder and single crystal samples. These findings are inconsistent with an ^{14}N assignment. The alternate assignment of the 28.3 MHz signal to ^1H nuclei is more strongly supported.

As previously discussed, the $-\text{CH}_3$ group is rotating at 120 K to give an averaged isotropic proton coupling of ~ 1.0 mT (28 MHz). The free proton frequency is 14.5 MHz or about half this value (1.2×28 MHz = 14 MHz). This is a necessary condition for observing a signal predicted by case (iii); that is, $\nu_n + |A|/2 = 14.5$ MHz + $|(28 \text{ MHz})/2| \approx 28.3$ MHz. This means that the proton coupling in the solid must be nearly equal to a value of about 28 MHz; exactly as observed from the single crystal EPR data. This signal would not be expected at temperatures where motion of the methyl group is restricted. In fact, the signal is not observed at 4 K.

When the crystal was cooled to 4 K, the signal at 28.3 MHz disappeared and a new signal centered at 14.5 MHz was observed consisting of two pairs of peaks, flanking a central peak, Figure 4c. The hyperfine couplings measured from the spectra are 0.08 mT (2.3 MHz), labeled *; 0.04 mT (1.1 MHz), labeled †; and <1 MHz (center peak). These peaks are assigned to small proton hfc interactions or to matrix proton signals as described in section VI.

There are two possibilities for the assignments of the couplings in Figure 4c: small proton hyperfine couplings from the two protons on the aromatic ring, or matrix ENDOR signals. Although the two ring protons have nearly identical hfc values, their principal axes are not coincident. Because of this, two pairs of ENDOR

peaks are expected corresponding to case (i) discussed previously. The Hamiltonian for ^1H in an oriented system is given by:

$$H = g_s \cdot \beta_s \cdot \mathbf{H} \cdot \mathbf{S} - g_n \cdot \beta_n \cdot \mathbf{H} \cdot \mathbf{I} + \mathbf{S} \cdot \mathbf{A} \cdot \mathbf{I} \quad (2)$$

Ignoring second order hyperfine terms and expressing the energy in Hertz, Equation (2) leads to an expression for the EPR transitions as:

$$E/h (m_s, m_I) = \nu_s m_s - \nu_n m_I + A m_s m_I \quad (3)$$

where $\nu_i = g_i \beta_i H/h$ and $i = s$ or n where s denotes the electron frequency and n the nuclear frequency; h = Planck's constant; β_s = electron Bohr magneton; β_n = nuclear Bohr magneton; and m_s and m_I are the spin quantum numbers.

From Equation (3) one can calculate the energy levels and ENDOR transitions as a function of frequency. A single calculation was carried out assuming no Fermi-Segré contact interaction for hfc interactions, i.e., purely dipolar interactions, and using the geometry shown in Figure 5. For this calculation the nitrogen of the nitroxyl group and the ring protons were assumed to be planar with the following bond lengths: C—N, 0.148 nm; C—C, 0.138 nm; and C—H, 0.108 nm. The coordinates in Figure 5 give the atomic positions in units of Å (nm ÷ 10) relative to the N—O• functional group, taken as the origin. For this geometry, the frequencies of ring proton ENDOR transitions were calculated. These values are plotted as the shift in frequency ($\Delta\nu$) from the free proton frequency (i.e., 14.5 MHz) as a function of orientation of \mathbf{B}_0 in the $Z'X'$ plane (Figure 5) (Note: Z' and X' do not coincide with the Z and X axes of Figure 2. Z' is $\sim 70^\circ$ from the Z axis in Figure 2). As shown by the arrow in Figure 5, for \mathbf{B}_0 at a position near the Z' axis (which coincides with our crystal orientation for the spectrum in Figure 4) the ENDOR transitions cross over, resulting in two closely positioned sets of peaks. These calculated frequencies correspond very well with the sets of peaks labeled * in Figure 4c. When the ENDOR experiment was repeated using a polycrystalline sample, only a single peak with a linewidth of 0.75 MHz was observed at 14.5 MHz. In the polycrystalline samples no signals corresponding to * were observed. Based on these findings, the lines labeled * in Figure 4c are assigned to the two ring proton couplings. The center peaks are assigned to a matrix ENDOR signal.

Matrix ENDOR signals are due to dipolar interactions between a trapped electron, hydrogen atom, or paramagnetic ion or fragment and the surrounding nuclei of the matrix. The signals contain information about the magnetic environment of the trapped species. A semiquantitative theory describing the matrix proton signal has been reported by Leniart, Hyde, and Vendrine,¹⁴ and has been discussed by Kevan and Kispert.¹³ In solids, the lineshape is due to nuclear spin relaxation which induces electron spin relaxation or due to motionally modulated dipolar interactions of the surrounding nuclei with the unpaired electron site. When the correlation time of the radical motion in the trapped site (τ_c) is much less than the electron spin lattice relaxation time (T_{1e}), the nuclear relaxation is dominated by motional fluctuations of the lattice. The matrix ENDOR spectrum of a trapped electron

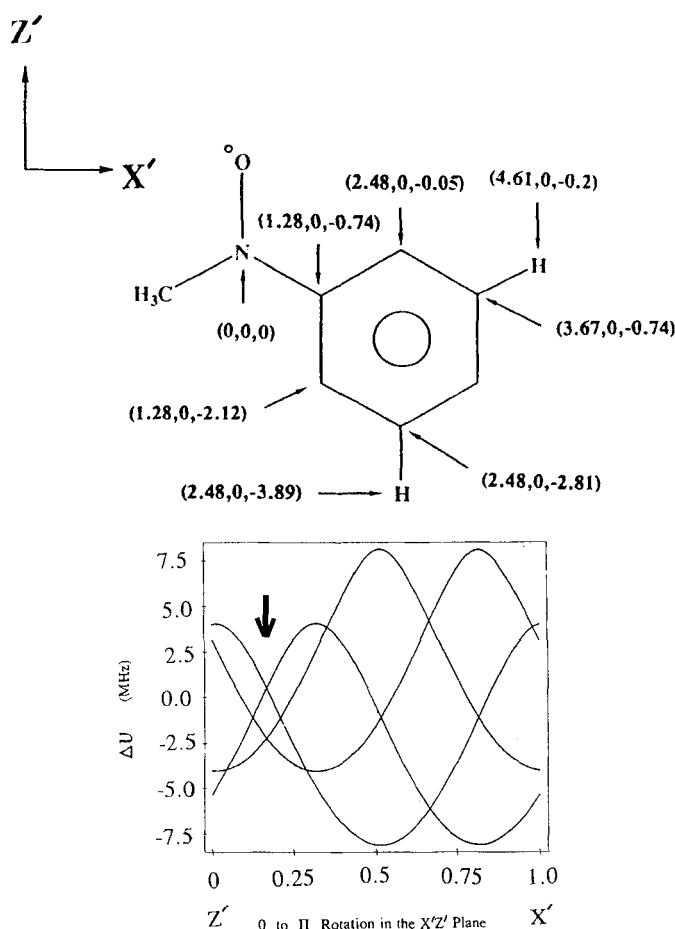


FIGURE 5 This figure shows the calculated shift of the aromatic ring protons' ENDOR lines from the free proton frequency versus the orientation of \mathbf{B}_0 in the $X'Z'$ plane. (Note: $X'Z'$ do not correspond to the XZ axes in Figure 2.) The position of \mathbf{B}_0 indicated by the arrow corresponds to the crystal orientation of the EPR spectrum in Figure 4(a). The observed ENDOR signals at 4 K in Figure 4(c) match very closely the predicted frequency shift. This supports the assignment of the peaks labeled * to the ring protons. The coordinates of the atomic positions used in the calculation are measured in Å relative to the $X'Z'$ plane.

interacting with surrounding nuclei can be calculated by varying the distance of the unpaired electron from a single proton nucleus by using the lineshape equation,¹⁴

$$f(\omega, r_i) = k\omega T_m^{-1}(\theta, r_i) \exp - [(\omega_Z + \omega_{FC} + \omega_D - \omega_0)^2 / (T_2^{-1})^2] r_i^2 \sin \theta d\theta \quad (4)$$

where k is a scaling factor; $T_n(\theta, r_i)$ is the nuclear relaxation of the i th proton, ω_z is the electron Zeeman frequency, $\omega_D(\theta, r_i)$ is the dipolar interaction between the trapped electron and the proton nucleus and ω_{FC} is the proton hyperfine coupling. T_2 is the electron spin-spin relaxation time; r_i is the electron-nuclear distance and

θ is the deviation of r_i from the applied magnetic field direction. Using this equation, we have calculated the matrix ENDOR pattern for cases where $\omega_D < T_2^{-1}$ (a single peak), $\omega_D > T_2^{-1}$ (a doublet), and $\omega_D \gg T_2^{-1}$ (a doublet with shoulders) as described in Reference 14. The superposition of these peaks with $T_2^{-1} = 10$ kHz and $\omega_{FC} = 50$ kHz closely corresponds with the lineshape of the center peak and peaks labeled † in Figure 4c as shown by the inset in Figure 4c. These ENDOR signals show that the trapped paramagnetic species differ from (I).

VI. DISCUSSION

Understanding sensitivity of energetic materials is a complex problem because there are many contributing factors, including: molecular structure, crystal structure, impurities, defects, density, polymorphism, particle size, temperature, pressure, and trigger linkages (weak bonds). To measure sensitivities of energetic materials, a standardized impact test is used. This test consists of dropping a weight (usually 2.5 kg) from increasing heights onto an energetic sample. The height which gives 50% probability of detonation is conventionally reported as the sensitivity indicator.

Tetryl is an insensitive energetic material. The drop height of tetryl varies from 26–32 cm. On the other end of the scale, lead azide is very sensitive, 2–4 cm. Impact sensitivities have been correlated with structure, by Kamlet and Adolph,⁴ using an oxygen balance. However, most attempts to explain sensitivity neglect chemical processes such as radical formation and decay. An acyclic nitroxyl radical has the general structure $R_1-(\text{NO}\bullet)-R_2$. For (I), $R_1 = -\text{CH}_3$ and $R_2 = -\text{C}_6\text{H}_2(\text{NO}_2)_3$. In the crystal, formation of this radical by cleavage of the nitramine bonds is facilitated by hydrogen bonding of the NO_2 group. The crystal structure data indicate that restriction of motion of one of the NO_2 oxygens occurs due to hydrogen bonding perpendicular to the NO_2 plane. Once formed, the radical is stabilized by two contributing factors: (i) delocalization of unpaired spin density onto the aromatic ring and (ii) methyl group rotation. Although delocalization of unpaired electron density is significant, the p -orbital of the $-\text{NO}\bullet$ group of (I) is directed at an angle of $\sim 70^\circ$ with respect to the plane of the ring. This restricts the delocalized π spin distribution of the unpaired electron, since a planar configuration would maximize delocalization. The rotation of the methyl group may stabilize the radical because of the additional degrees of motional freedom it provides to the structure. From solution studies (I) is known to undergo loss of $\bullet\text{CH}_3$.² The identity of the counter radical formed subsequent to $\bullet\text{CH}_3$ loss is not known. In the solid the trapped methyl radical might account for the matrix ENDOR signal. Another possibility is trapped $\text{NO}\bullet$, a product of the nitro/nitroxyl rearrangement to form (I).

A recent study of sensitivity by Storm and co-workers¹⁵ compares a series of picryltriazone isomers having nitroaromatic rings similar to tetryl. Their calculations suggest that 1-picryl-1,2,3-triazole and 4-nitro-1-picryl-1,2,3-triazole eliminate N_2 to form nitrogen centered bi-radicals which would yield reaction products making these materials more sensitive to impact tests. If this proves correct, then their study shows how radicals can act as sensitizers. Our findings in tetryl suggest a

converse relationship. The stability of (I) and the enhanced degrees of freedom of the rotating methyl group may be desensitizing factors in tetryl. As more information about free radical stabilization in energetic materials is learned, correlations with sensitivity can be made. The brief data now available suggest that stable radical products in energetic materials may be *indicators* of sensitivity, as well as participants in decomposition.

VII. SUMMARY

Tetryl forms a nitroxyl radical in the single crystal phase retaining the atomic geometry of the parent molecule. This is supported by the excellent match of experimental EPR spectra and computed spectra which are based on the crystal structure coordinates. The methyl group of radical (I) is rotating in the solid state with a frequency greater than 30 MHz at 120 K. The ENDOR spectra at 120 K confirm methyl group rotation. At 4 K a matrix ENDOR signal is observed. The matrix ENDOR spectra of the trapped paramagnetic species can be explained according to the theory of Leniart, Hyde, and Vedral.¹⁴ The highly stable nature of (I) in tetryl and the low sensitivity of tetryl to impact tests suggests the following hypothesis: *Energetic materials with nitramine groups which, by the elimination of NO₂, can form stable nitroxyl radicals in the solid-state will be less sensitive than those materials which cannot form stable nitroxyl radicals.*

Acknowledgments

The Office of Naval Research is acknowledged for sponsorship of one of the authors (MDP) under the Energetic Materials Program of Dr. Richard S. Miller. Dr. J. Sharma of the Naval Surface Warfare Center, White Oak, MD, provided the tetryl used for some of the experiments. Bruker Instruments is acknowledged for ESP300 ENDOR spectra recorded at Billerica, MA. Dr. L. Piekara-Sady at the University of Alabama, Tuscaloosa, AL (on leave from the Inst. of Mol. Phys., Poznan, Poland) is acknowledged for ENDOR of the polycrystalline samples. Dr. D. A. Dutt (NRL) assisted with the Q-band measurements.

References

1. T. Urbanski, *Chemistry of Technology of Explosives (Vol. III)*, M. Jurecki, S. Laverton, editors; Pergamon Press, (1967).
2. F. J. Owens, *Mol. Cryst. Liq. Cryst.*, **126**, 379 (1985).
3. M. J. Kamlet, *Proceedings of the Sixth Symposium (International) on Detonation*, San Diego, California, Aug. 24–27, 1976. ONR Report ACR 221, p. 312.
4. M. J. Kamlet and H. G. Adolph, *Propellants and Explosives*, **4**, 30 (1979).
5. H. H. Cady, *Acta Cryst.*, **23**, 601 (1967).
6. M. D. Pace, W. R. Barger, and A. W. Snow, *Langmuir*, **5**, 973 (1989); M. D. Pace and S. M. Masumura, NRL Memorandum Report No. 6417, 1988.
7. M. D. Pace, A. D. Britt, and W. B. Moniz, *J. Energ. Mat.*, **1**, 127 (1983); A. D. Britt, M. D. Pace, and W. B. Moniz, *J. Energ. Mat.*, **1**, 367 (1983).

8. In the abc^* orthogonal reference frame, labeling the c^* axis indicates a difference from the c axis of the monoclinic unit cell direction of tetryl. The a and b axes coincide with the unit cell axes, but the coordinates of the abc^* system differ from the monoclinic abc system according to the following standard transformations: $a = a - c \sin (\beta - 90^\circ)$; $b = b$; $c = c \cos (\beta - 90^\circ)$; where abc refer to monoclinic coordinates, abc^* refer to orthogonal coordinates. β is the angle between the a and c monoclinic axes.
9. S. Schrier, C. F. Polnaszek, and I. C. P. Smith, *Biochimica et Biophysica Acta*, **515**, 375 (1978).
10. O. W. Maender, and E. G. Janzen, *J. Org. Chem.*, **34**, 4072 (1969).
11. H. M. Atherton, and B. Day, *Chem. Phys. Letters*, **15**, 428 (1972); A. H. Cohen and B. M. Hoffman, *J. Am. Chem. Soc.*, **95**, 2061 (1973).
12. B. Delley, P. Becker, and B. Gillon, *J. Chem. Phys.*, **80**, 4286 (1984).
13. L. Kevan, and L. D. Kispert, *Electron Spin Double Resonance Spectroscopy*, John Wiley and Sons, 1976, p. 7-10; p. 239-249.
14. D. S. Leniart, J. S. Hyde, and J. C. Vedrine, *J. Phys. Chem.*, **76**, 2079 (1972).
15. C. B. Storm, R. R. Ryan, J. P. Ritchie, J. H. Hall, and S. M. Bachrach, *J. Phys. Chem.*, **93**, 1000 (1989).